

Supporting information

Iridium complex-based ferroptosis inducer for cancer sonodynamic therapy

Guihong Ren^a, Qingxuan Meng^b, Panpan Li^a, Chenyi Wang^a, Chenglong Wu^a, Senqiang Zhu^{*a}, Yuhao Li^{*b}, Rui Liu^{*a}, Chenjie Zhu^c and Hongjun Zhu^a

^a*School of Chemistry and Molecular Engineering, Nanjing Tech University, Nanjing 211816, China.*

^b*School of Materials and Chemistry, Institute of Bismuth Science, Shanghai Collaborative Innovation Center of Energy Therapy for Tumors, University of Shanghai for Science and Technology, Shanghai 200093, China.*

^c*College of Biotechnology and Pharmaceutical Engineering, Nanjing Tech University, Nanjing 211816, China.*

**China E-mail:*

zhusenqiang1993@njtech.edu.cn (*Senqiang Zhu*)

yhli@usst.edu.cn (*Yuhao Li*)

rui.liu@njtech.edu.cn (*Rui Liu*)

Contents

Experimental Section

Scheme S1. Synthesis scheme for complex **Ir-1**.

Figure S1. ^1H NMR spectrum of **L1**.

Figure S2. ^1H NMR spectrum of **Ir-1**.

Figure S3. ^{13}C NMR spectrum of **Ir-1**.

Figure S4. HRMS spectrum of **Ir-1**.

Figure S5. UV-vis spectra of **Ir-1** in different solvents.

Figure S6. The HOMO and LUMO distributions of **Ir-1**.

Figure S7. Triplet excited state lifetime of **Ir-1**.

Figure S8. Emission spectra of **Ir-1** in DCM solution under nitrogen and air atmosphere.

Figure S9. Thermogravimetric analysis (TG) results of **Ir-1**.

Figure S10. The absorption spectra of **Ir-1** in different pH values.

Figure S11. Absorbance attenuation of DPBF by ROS generation after treatments.

Figure S12. Absorbance attenuation and degradation rate curve of DPBF after treatments.

Figure S13. The $\cdot\text{OH}$ by DMPO and **Ir-1** upon US irradiation detected by ESR spectroscopy.

Figure S14. Standard curve of the area under the curve with MDA concentration.

Figure S15. Fe^{2+} fluorescence imaging of 4T1 cells in different groups.

Figure S16. Cytotoxicity of 4T1 cells in different groups.

Figure S17. Hemolytic analysis after the treatment of **Ir-1** with various concentrations.

Figure S18. The standard blood routine data of mice treated with **Ir-1** by intravenous injection 21 days.

Figure S19. H&E-stained sections of mice organs including heart, liver, spleen, lung, and kidney tissues.

Figure S20. Fluorescence images of 4T1 cells under various treatments.

Figure S21. Fluorescence intensities of 4T1 cells under various treatments.

Table S1. The electrochemical properties of **Ir-1**.

Experimental Section

Materials. All reagents that were purchased from commercial sources were analytical pure and used without further purification. 2-chloropyridine, Pd(PPh₃)₄, K₂CO₃, 5-hydroxypicolinic acid, anhydrous Na₂SO₄, 5,5-dimethyl-1-pyrroline-1-oxide (DMPO), 2,2,6,6-tetramethyl-4-piperidinone hydrochloride (TEMP), Ru(bpy)₃Cl₂ (Shanghai Bidie Pharmaceutical Technology Co., Ltd., China), benzo[*b*]thiophen-2-ylboronic acid, 1,3-Diphenylisobenzofuran(DPBF) (Shanghai Titan Technology Co., Ltd., China), IrCl₃·3H₂O (J&K Scientific, China), 1,4-dioxane, phosphate buffered saline (PBS), petroleum ether (PE), ethyl acetate (EA), dimethyl sulfoxide (DMSO), methanol (MeOH), ethanol (EtOH), dichloromethane (DCM), acetonitrile (MeCN).

Instruments. ¹H NMR, ¹³C NMR spectra were obtained using a Bruker-400 MHz NMR spectrometer using DMSO-*d*₆ as the solvent. ESI-HRMS analysis was performed by matrix-assisted laser desorption/ionization-time of flight mass spectroscopy (MALDI-TOF). The ultraviolet to visible (UV-vis) absorption spectra and fluorescence/phosphorescence emission spectra were acquired by a TU-1900 UV and Hitachi-F-4600 fluorescence spectrophotometer, respectively. Nanosecond transient absorption (TA) spectra and triplet excited state lifetime were recorded on LP980 laser flash photolysis spectrometer. The electron spin resonance (ESR) measurements were carried out with a Bruker Model A200 spectrometer. The cell viability assay was measured by a Thermo fisher Multiskan MK3 microplate reader. Fluorescence images of the stained cells were taken using a Nikon TS100 inverted fluorescence microscope. Intracellular lipid peroxide (LPO) staining images were screened by a ZEISS LSM 700 confocal laser scanning microscope (CLSM).

Synthesis

Synthesis of L1. Benzo[*b*]thiophen-2-ylboronic acid (0.862 g, 4.844 mmol), Pd(PPh₃)₄ (0.407 g, 0.352 mmol), K₂CO₃ (3.043 g, 22.02 mmol) and 2-chloropyridine (0.5 g, 4.404 mmol) were added into a 100 mL two-mouth flask followed by water (10 mL)

and 1,4-dioxane (30 mL) in the flask. Nitrogen was pumped into the reaction system three times, followed by reflux reaction for 16 h, and the system gradually changed from yellow suspension to clarified solution. After the reaction was over, the mixed system was cooled to room temperature, the reaction liquid was extracted, washed and dried to obtain organic phase, and the crude product obtained by vacuum distillation was subsequently purified via column chromatography (PE:EA = 15:1 v/v) to get a white solid (0.501 g, 2.371 mmol, 77% yield). **¹H NMR** (400 MHz, DMSO-*d*₆) δ 8.62 (ddd, *J* = 4.9, 1.9, 0.9 Hz, 1H), 8.19 (s, 1H), 8.12 (dt, *J* = 8.0, 1.1 Hz, 1H), 8.02-7.97 (m, 1H), 7.95-7.85 (m, 2H), 7.45-7.34 (m, 3H).

Synthesis of Ir-1. A mixture of [Ir(C^N)₂Cl]₂ (0.500 g, 0.386 mmol), 5-hydroxypicolinic acid (0.134 g, 0.965 mmol), K₂CO₃ (0.587 g, 4.246 mmol), DCM (30 mL), EtOH (10 mL) was added to a two-necked flask (100 mL) and heated at 60 °C overnight under argon. The system was observed to be a dark orange turbid liquid. Upon completion of the reaction, the crude product was acquired by removing the solvent. And then further purifying by silica gel column chromatography (DCM:MeOH = 20:1, v/v) and DCM trituration, giving the desired compound. orange powder (125 mg, 0.166 mmol, 43% yield). **¹H NMR** (400 MHz, DMSO-*d*₆) δ 11.13 (s, 1H), 8.58 (d, *J* = 5.8 Hz, 1H), 8.06-7.81 (m, 7H), 7.63 (d, *J* = 5.8 Hz, 1H), 7.41 (dd, *J* = 8.7, 2.6 Hz, 1H), 7.34 (ddd, *J* = 7.4, 5.8, 1.5 Hz, 1H), 7.24-7.11 (m, 4H), 6.86 (dt, *J* = 26.6, 7.6 Hz, 2H), 6.13 (d, *J* = 8.1 Hz, 1H), 5.91 (d, *J* = 8.1 Hz, 1H). **¹³C NMR** (101 MHz, DMSO) δ 172.85, 165.09, 164.43, 158.69, 150.05, 149.05, 148.16, 146.74, 145.86, 145.71, 142.49, 142.05, 140.08, 137.21, 135.83, 134.78, 129.70, 126.11, 125.66, 125.33, 125.20, 124.98, 124.56, 124.34, 123.79, 123.54, 121.69, 121.12, 119.55, 119.31. **HRMS** (ESI) m/z calcd for C₃₂H₂₀IrN₃O₃S₂⁺ (M)⁺ 751.0575, found 752.0632.

Density Functional Theory

The density functional theory (Density Functional Theory, DFT) was employed to calculate the complexes **Ir-1**. All calculations were conducted using Gaussian software. The metal atoms were calculated with the LanL2DZ basis set, while other atoms were

calculated with the 6-31G(d,p) basis set. Geometric optimization was carried out based on these calculations. The optimized geometries of all complexes were calculated under vacuum conditions.

Sonodynamic performance measurements

The mixture solution of 20 μg DPBF and **Ir-1** (10 $\mu\text{g mL}^{-1}$, 5.0 mL) was exposed to different US irradiation (2.5 W cm^{-2}) for 5 min, and the absorbance of DPBF at 410 nm was recorded to measure ROS generation. For ESR measurements, the mixture solution of 20 μL TEMP and **Ir-1** (10 $\mu\text{g mL}^{-1}$, 5.0 mL) was exposed to US irradiation for 5 min, and the signal of $^1\text{O}_2$ was detected by ESR spectrometer using TEMP as the trapping agent.

Cell culture

Mouse breast cancer (4T1) cells were purchased from the Shanghai Institute of Biochemistry and Cell Biology. 4T1 cells were cultured in RPMI-1640 (Sigma, USA) containing 10% fetal calf serum (FBS, Gibco, ThermoFisher) and 1% penicillin-streptomycin (Gibco, ThermoFisher). All cells were grown in a humid incubator (ThermoFisher, USA) at 37 $^{\circ}\text{C}$. The gas consists of 5% carbon dioxide and 95% air.

Cell proliferation assay

For dark toxicity, the cell suspension was seeded into a 96-well plate with 5,000 cells in each well and then incubated for 24 h. The RPMI-1640 culture medium (100 μL) containing **Ir-1** with the concentration of 0, 10, 20, 30, 40, 50 $\mu\text{mol L}^{-1}$ were added and cultured in an incubator for 24 h and 48 h. For sonodynamic toxicity, the concentration of **Ir-1** was the same as dark toxicity. After **Ir-1** incubated 4T1 cells for 24 h, US with a power density of 0.7 W cm^{-2} for 3 or 5 min was applied. Next, cell viability was determined by cell counting kit-8 (CCK-8, Beyotime Biotechnology, China). The experiment was carried out according to the manufacturer's instructions. Add 90 μL cell culture medium and 10 μL CCK-8 solution to each well, incubate in the incubator

for 1.5 hours, and measure the absorbance at 450 nm using a BioTek microplate reader (Thermo Fisher Scientific, USA). Five replicates were conducted for each concentration to reduce the randomness of the experiment ($n = 5$). Cell survival rate = $[(\text{As-Ab})/(\text{Ac-Ab})] \times 100\%$, where As is the experimental group, Ac is the control group, and Ab is the blank group.

Assays for intracellular ROS production

Intracellular ROS production was detected using a reactive oxygen species detection kit (DCFH-DA fluorescent probe, Beyotime Biotechnology, China). 4T1 cells were seeded into 24-well plates at a density of 5×10^4 cells per well and incubated for 24 h. **Ir-1** ($55 \mu\text{g mL}^{-1}$) was then dispersed in RPMI-1640 and added to groups **Ir-1** and **Ir-1 + US**, which were further incubated for 24 h. Subsequently, cells in groups US and **Ir-1 + US** were subjected to US stimulation and then incubated for an additional 6 h. DCFH-DA was added according to the manufacturer's instructions, and the cells were incubated in the dark for 30 min. Finally, cells were washed twice with PBS and observed using an inverted fluorescence microscope (Olympus IX73, Japan) to visualize the staining results (DCFH-DA: green).

Calcein-AM/PI staining

2×10^4 cells/well of 4T1 cells were seeded on a 24-well plate for 12 h and then treated with pure fresh or material-containing ($55 \mu\text{g mL}^{-1}$ **Ir-1** RPMI-1640 medium (300 μL)). Cells in some groups were treated by the US after incubation for another 24 h. The dead and living cells were detected with a Calcein-AM/PI kit (Beyotime, China). Before staining, the supernatant was discarded, and the cells were washed thoroughly with buffer three times. Then, Calcein-AM solution (2 mM, 5 μL) and PI solution (1.5 mM, 15 μL) were added to a 24-well plate and incubated with cells at 37°C for 30 min. Living cells (green fluorescence) and dead cells (red fluorescence) were simultaneously detected by a fluorescence microscope.

Mitochondrial damage evaluation

Mitochondrial membrane potential damage was assessed using the JC-1 kit (C2006, Beyotime Biotechnology, China). JC-1 accumulates in the mitochondrial matrix in cells with high membrane potential, emitting red fluorescence. When the membrane potential is disrupted, JC-1 exists as monomers emitting green fluorescence. Treat the four groups of cells according to the above-mentioned conditions. After an additional 24 h of incubation, cells were washed with PBS and stained with a mixture of 0.3 mL JC-1 staining solution and 0.3 mL RPMI-1640 medium for 20 min at 37°C, then washed with JC-1 washing solution. Fluorescence microscopy was used to observe the changes in mitochondrial membrane potential in different groups.

Detection of malondialdehyde

Malondialdehyde (MDA) levels were measured using an MDA detection kit (Beyotime, China) to evaluate lipid peroxidation (LPO) levels. 4T1 cells were seeded into 24-well plates at a density of 5×10^4 cells per well and incubated for 24 h. **Ir-1** (55 $\mu\text{g mL}^{-1}$) was then dispersed in RPMI-1640 and added to groups **Ir-1** and **Ir-1 + US**, which were further incubated for 24 h. Cells in groups US and **Ir-1 + US** were subjected to US stimulation and incubated for an additional 12 h. Cells were then collected and lysed on ice, and the supernatant was obtained by centrifugation. The supernatant was mixed with MDA detection reagent according to the manufacturer's instructions and heated at 100°C for 20 min. After cooling to room temperature, the sample was centrifuged, and the absorbance was measured at 532 nm.

Detection of intracellular lipid droplets

Intracellular lipid droplets were detected using a lipid droplet green fluorescence detection kit (BODIPY, Beyotime, China). 4T1 cells were seeded into 6-well plates at a density of 1×10^5 cells per well and incubated for 24 h. Ir-1 (55 $\mu\text{g mL}^{-1}$) was then dispersed in RPMI-1640 and added to groups **Ir-1** and **Ir-1 + US**, which were further incubated for 24 h. Cells in groups US and **Ir-1 + US** were subjected to US stimulation

and incubated for an additional 12 h. Cells were then washed twice with PBS, stained with the staining solution according to the manufacturer's instructions, and incubated in the dark at 37°C for 15 min. Finally, cells were washed twice with PBS and observed using an inverted fluorescence microscope to visualize the staining results (green fluorescence).

Tumor model

The six-week-old Balb/c female mice used for establishing the 4T1 tumor model were obtained from the Laboratory Animal Management Department, Shanghai Family Planning Research Institute authorized by the Shanghai Laboratory Animal Quality Supervision and Inspection Station (SCXK 2018-0006). In detail, the 4T1 cell suspension (2×10^6 cells mL^{-1} , 100 μL) was injected into the axilla of the hind leg of mice. About 7 days later, the 4T1 tumor model was used for the following studies. All animal experiments were conducted in the Shanghai Ruitaimosi Biotechnology Co., Ltd. authorized by the Shanghai Science and Technology Committee (SYXK 2021-0007) and under the guidelines of the Institutional Animal Care and Use Committee of Shanghai Shidong Hospital (2023-036-01).

Sonodynamic therapy in vivo

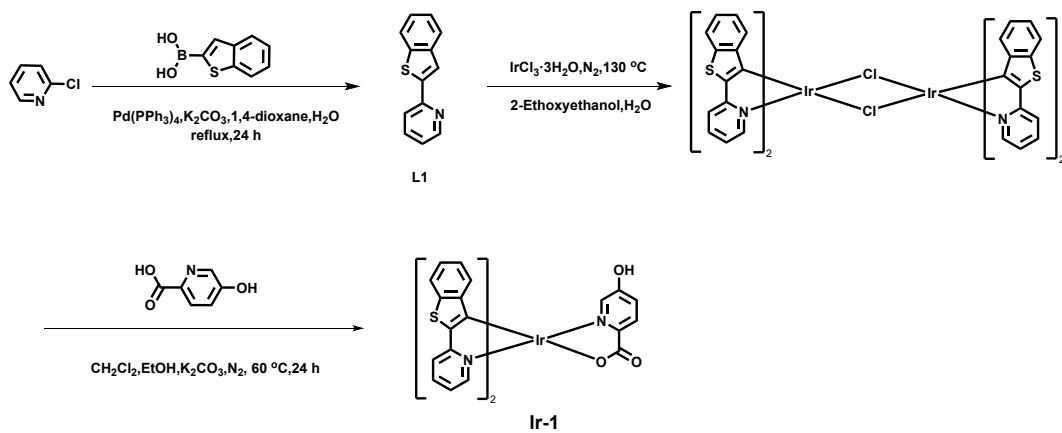
Tumor-bearing mice were randomly assigned to four groups: (1) control, (2) US, (3) **Ir-1**, (4) **Ir-1+US** (2 mg mL^{-1} ; US: 0.7 W cm^{-2} for 5 min). Groups (1) and (2) received intravenous injections of PBS. Twelve hours after injection, groups (2) and (4) were subjected to US. The mice underwent two treatments during the 15-day treatment period. After 24 h of US treatment, one mouse from groups (1) and (4) was euthanized. They were treated on the first and third days. The mice's tumor volume and body weight were recorded every three days. The tumor volume was calculated as follows: $V = 0.52 \times \text{length} \times \text{width}^2$. The tumors were removed, captured on camera, and weighed when the mice were put down fifteen days later. The tumors in each group were then divided into tissue slices and stained with H&E to conduct histological analysis.

Hemolytic test

Mice blood (1 mL) was collected from the mouse eyeball and then diluted with 2 mL PBS. After 1 h, the mixture was centrifuged (1,200 rpm for 5 min). The obtained red blood cells were dispersed in 4 mL PBS. Red cell suspensions were incubated with concentrations of 0, 5, 10, 25, 50, 75, 100 $\mu\text{g mL}^{-1}$ **Ir-1**, PBS, and deionized water. After incubating for five hours, the mixture was centrifuged (13,500 rpm, 10 min) to obtain the supernatant and measure the absorbance values of each group at 570 nm. The hemolysis rate of red blood cells is calculated as follows: Hemolysis rate (%) = $(A_{\text{sample}} - A_{\text{PBS}}) / (A_{\text{water}} - A_{\text{PBS}}) \times 100\%$.

Hematologic analysis

Ir-1 (2 mg mL^{-1} , 200 μL) was intravenously injected into Balb/c mice, and blood samples were taken on day 1 and day 21 for various blood indicators. Then, the heart, liver, spleen, lung, and kidney were fixed in formalin solution and sectioned for H&E staining.



Scheme S1. Synthesis scheme for complex **Ir-1**.

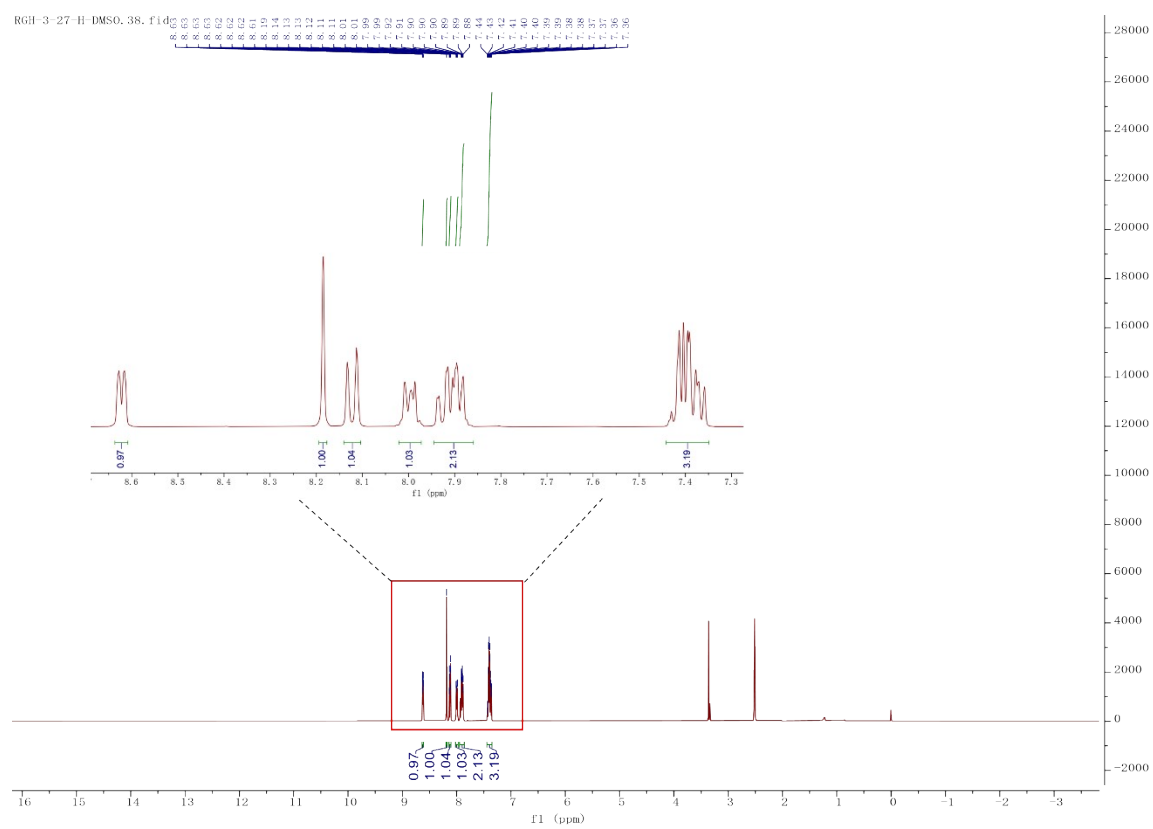


Fig. S1. ^1H NMR spectrum of L1.

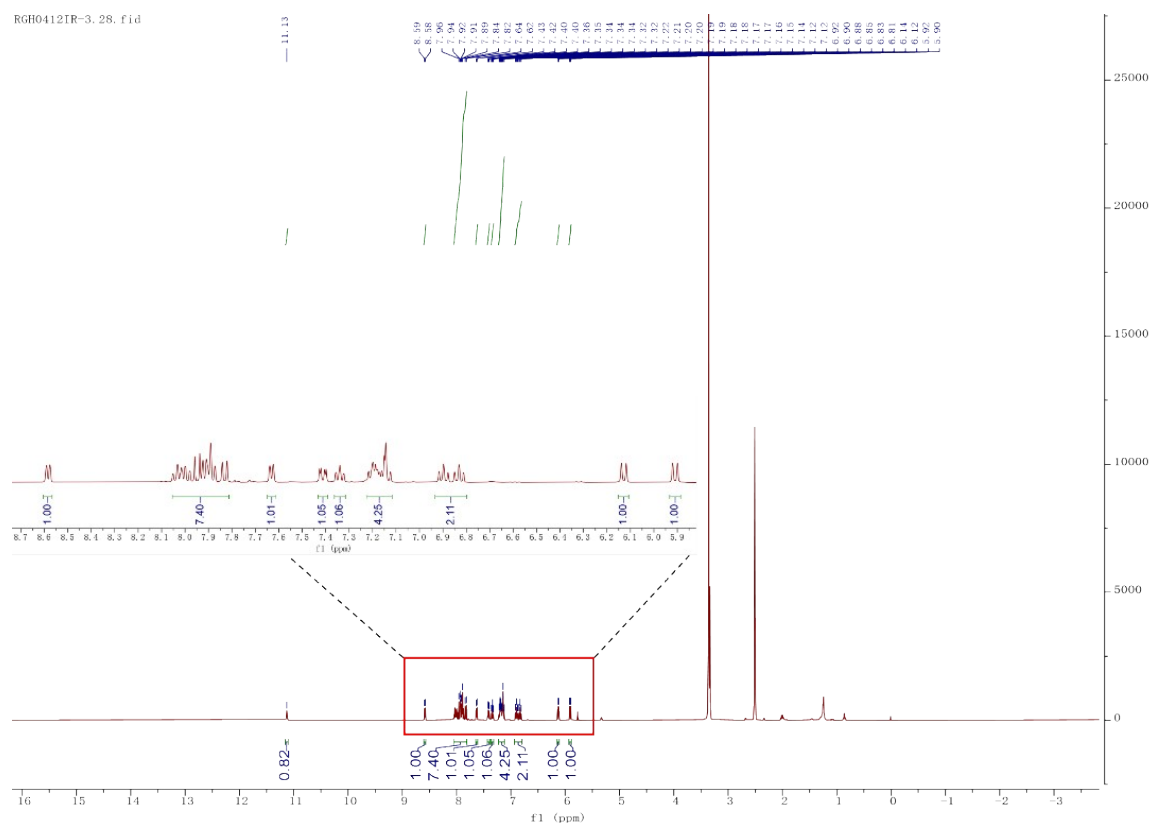


Fig. S2. ^1H NMR spectrum of Ir-1.

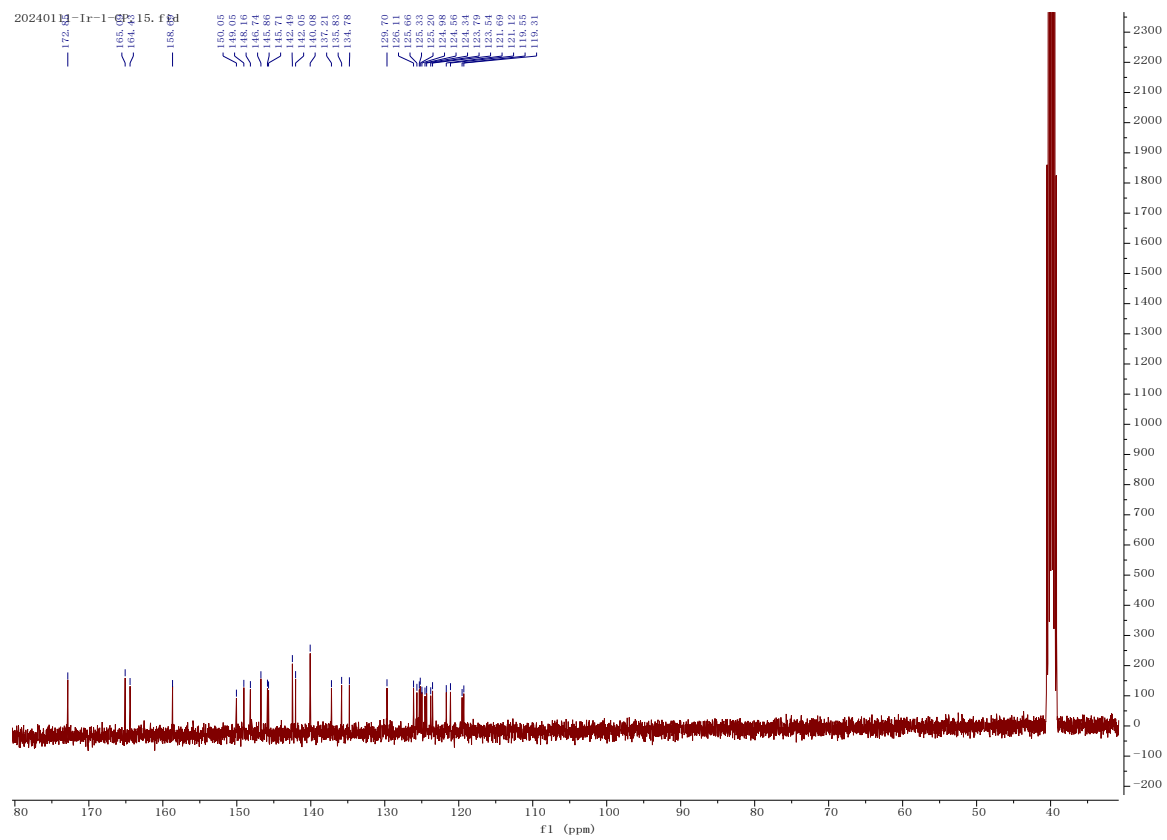


Fig. S3. ^{13}C NMR spectrum of Ir-1.

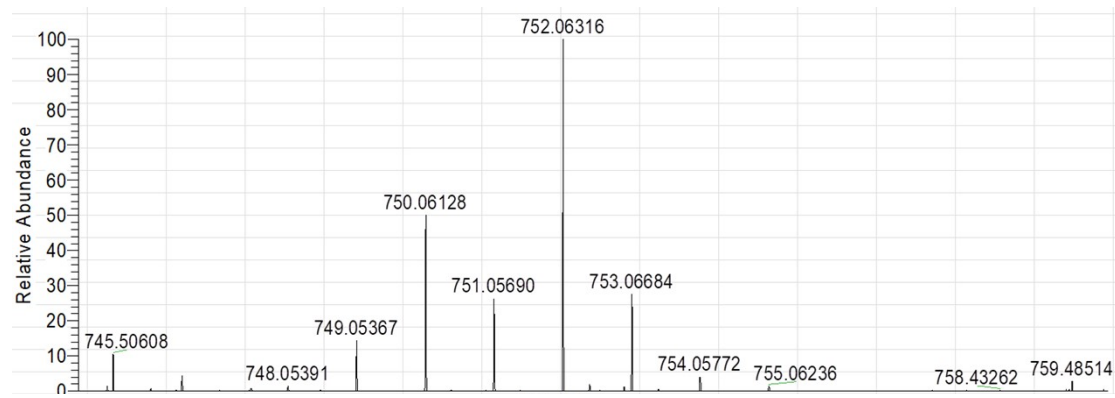


Fig. S4. HRMS spectrum of Ir-1.

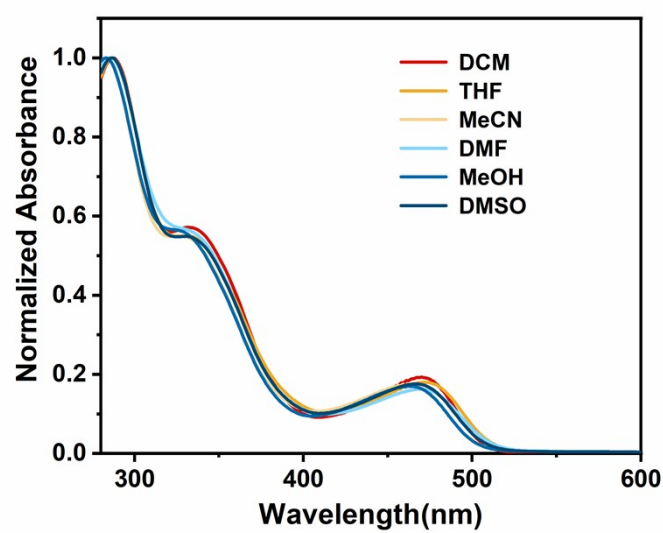


Fig. S5. UV-vis spectra of **Ir-1** in different solvents.

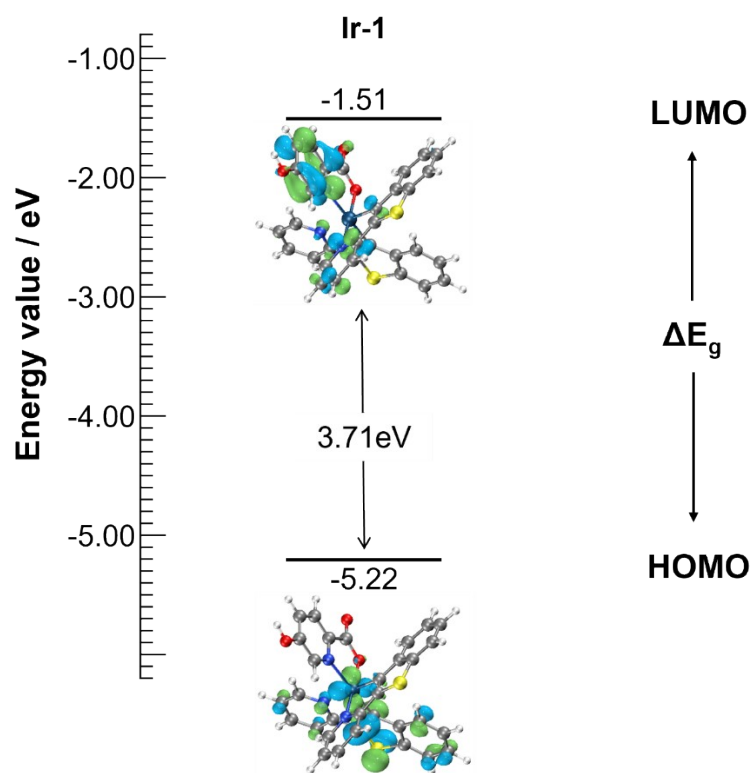


Fig. S6. The HOMO and LUMO distributions of **Ir-1**.

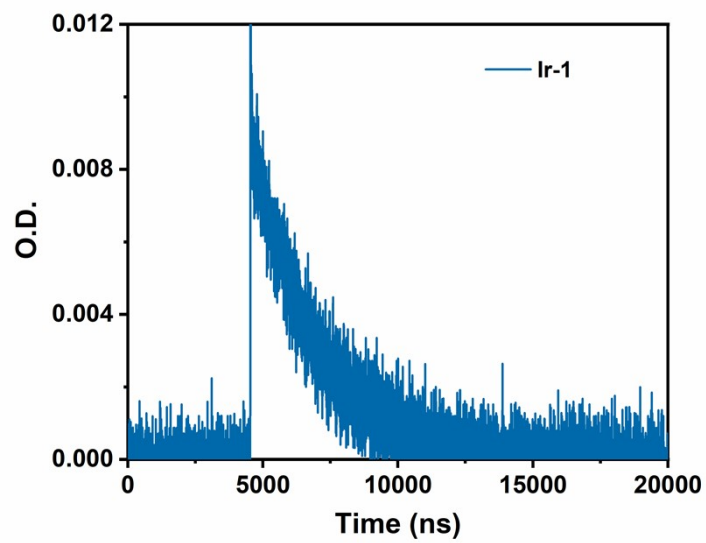


Fig. S7. Triplet excited state lifetime of **Ir-1** in DMSO at 298 K.

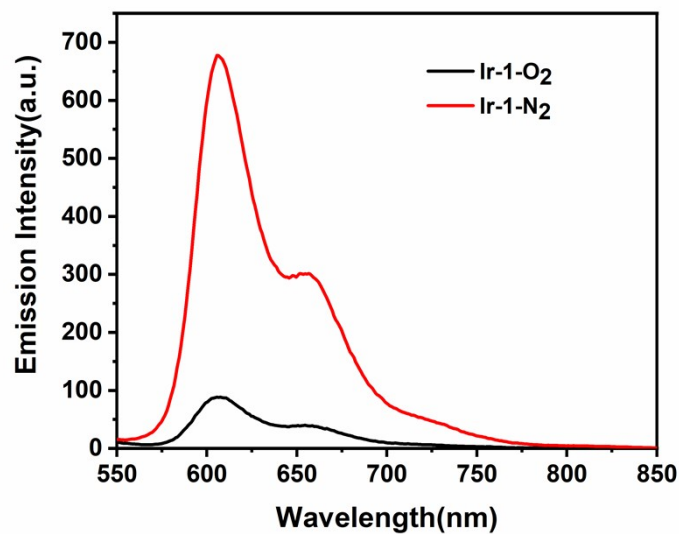


Fig. S8. Emission spectra of **Ir-1** in DCM solution under nitrogen and air atmosphere.

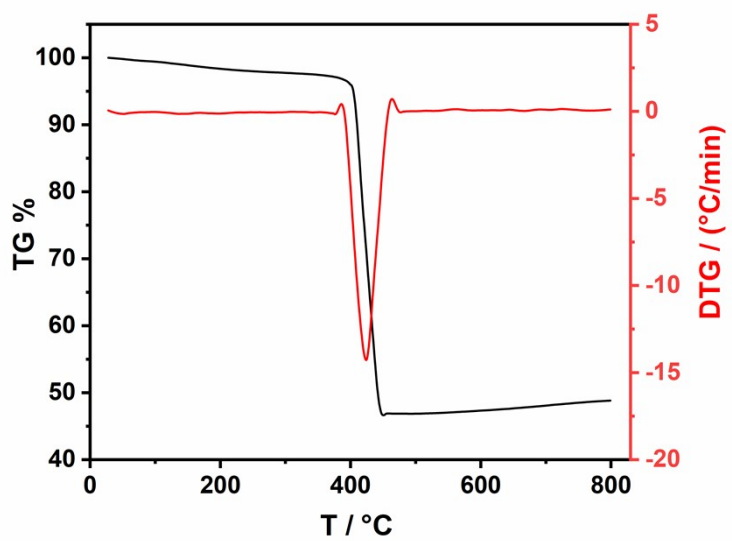


Fig. S9. Thermogravimetric analysis (TG) results of **Ir-1**.

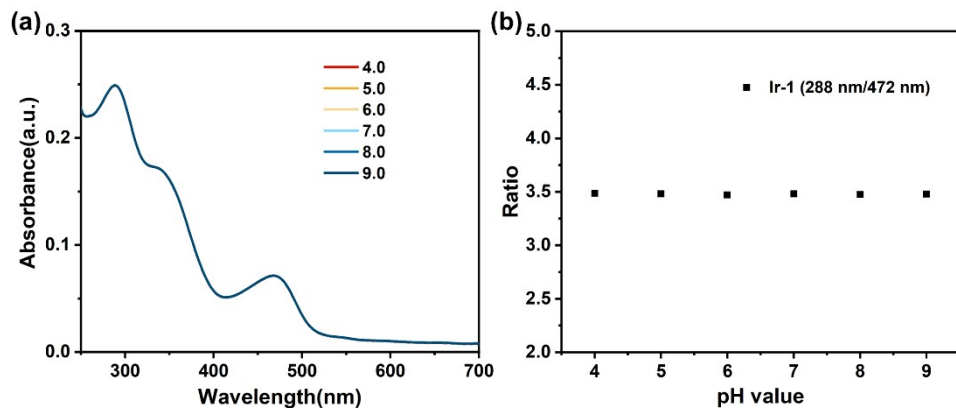


Fig. S10. (a) The absorption spectra of **Ir-1** in different pH values. (b) Absorption ratio of 288 nm/472 nm for **Ir-1** in different pH values.

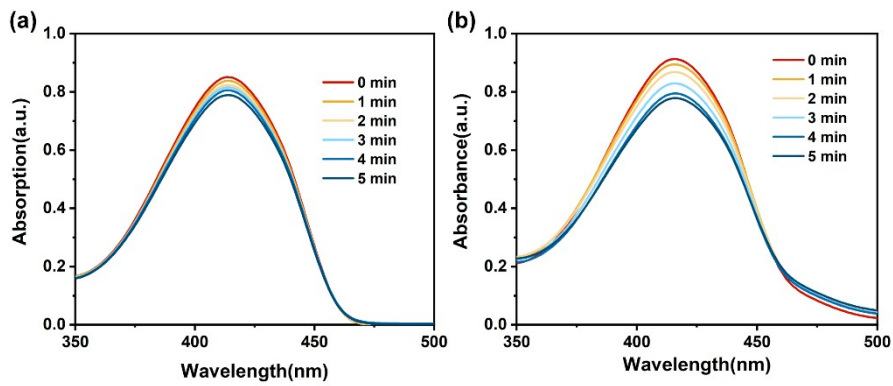


Fig. S11. (a) Absorbance attenuation of DPBF (10 μ M, DMF) by ROS generation following various irradiation durations. (b) Absorbance attenuation of DPBF (10 μ M, DMF) by ROS generation in the presence of Ru(bpy)₃Cl₂ (10 μ M) following various irradiation durations.

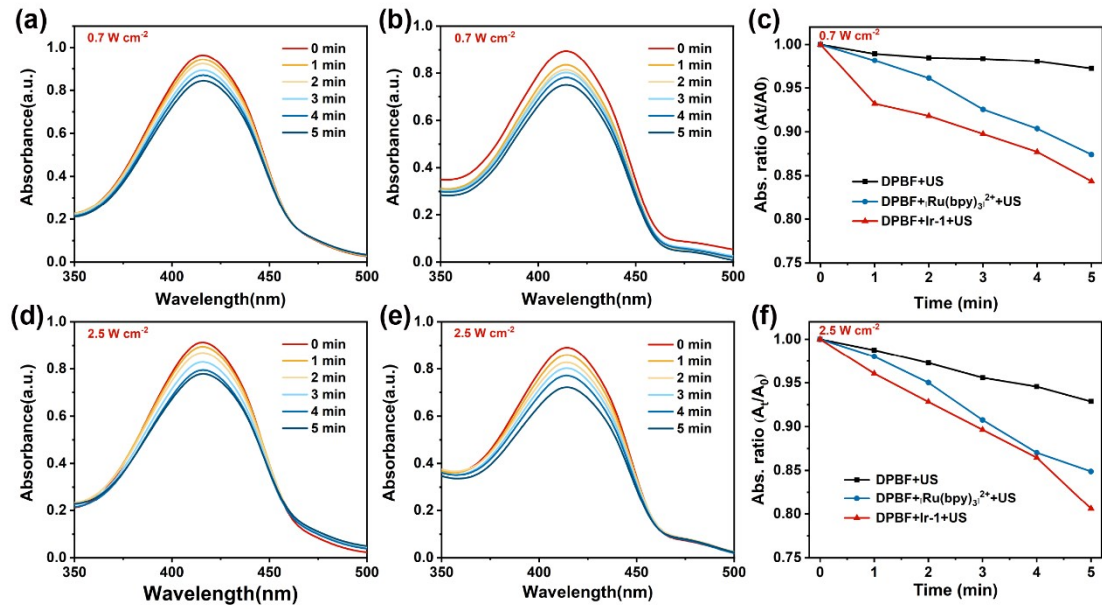


Fig. S12. (a-b) Absorbance attenuation of DPBF (10 μ M, DMF) by ROS generation in the presence of Ru(bpy)₃Cl₂ and **Ir-1** (10 μ M) following various irradiation durations (0.7 W cm⁻²). (c) Time-dependent absorption change at 410 nm (0.7 W cm⁻²). (d-e) Absorbance attenuation of DPBF (10 μ M, DMF) by ROS generation in the presence of Ru(bpy)₃Cl₂ and **Ir-1** (10 μ M) following various irradiation durations (2.5 W cm⁻²). (f) Time-dependent absorption change at 410 nm (2.5 W cm⁻²).

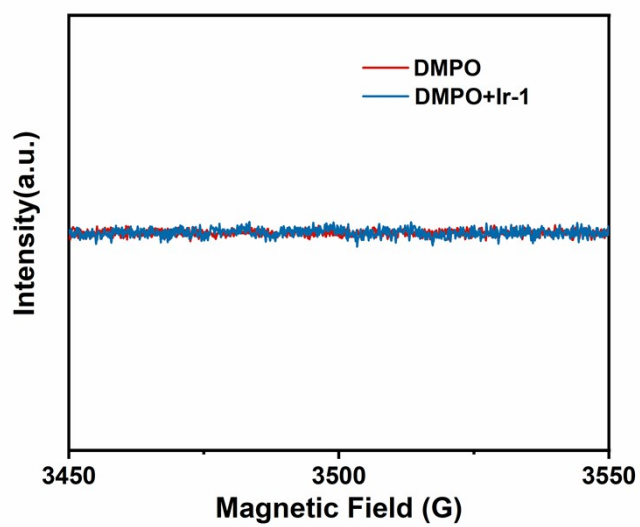


Fig. S13. The $\cdot\text{OH}$ by DMPO and **Ir-1** upon US irradiation detected by ESR spectroscopy.

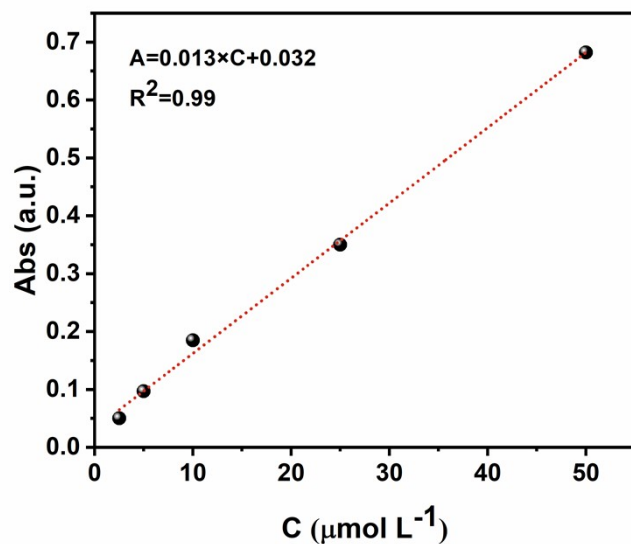


Fig S14. Standard curve of the area under the curve with MDA concentration.

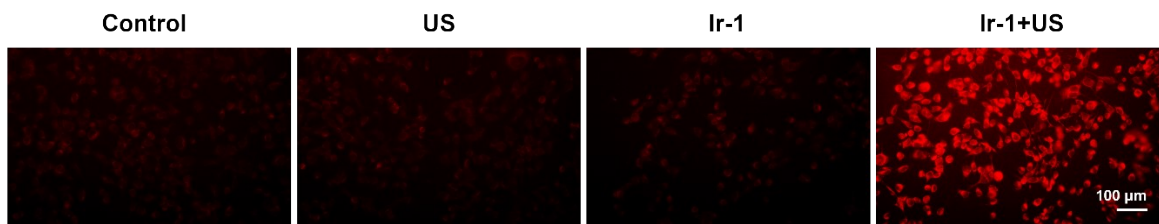


Fig S15. Fe^{2+} fluorescence imaging of 4T1 cells in different groups (0.7 W cm^{-2} , 5 min).

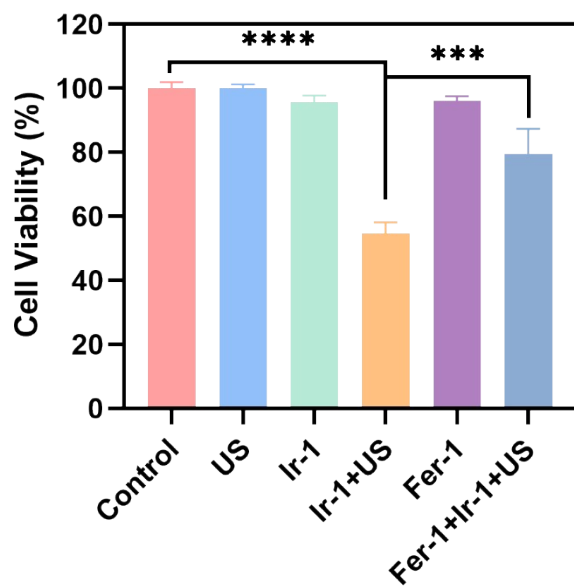


Fig S16. Cytotoxicity of 4T1 cells in different groups (0.7 W cm⁻², 5 min; n=3).

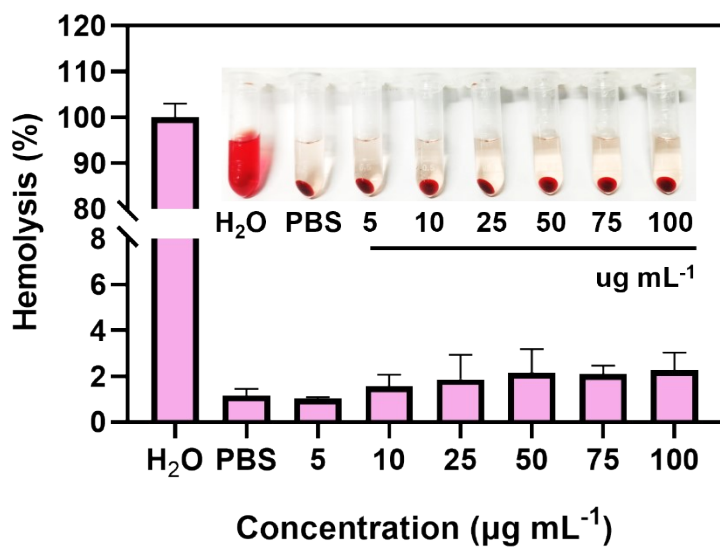


Fig S17. Hemolytic analysis and images of hemolysis of red blood cells after the treatment of **Ir-1** with various concentrations.

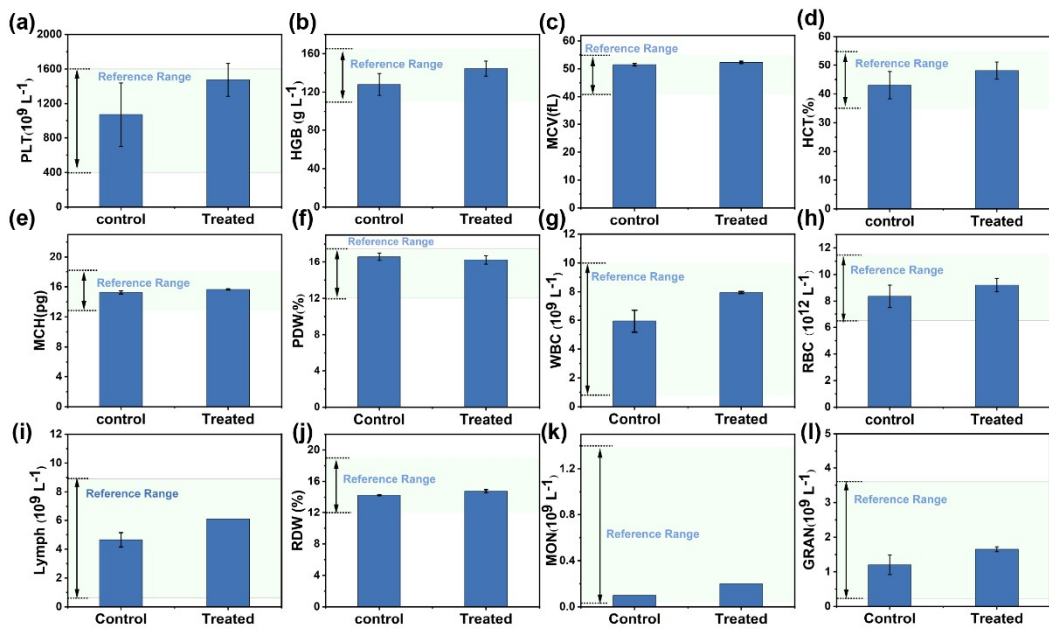


Fig S18. The standard blood routine data of mice treated with **Ir-1** (2 mg mL^{-1} , $200 \mu\text{L}$) and PBS (control) by intravenous injection 21 days. (a) Platelets (PLT); (b) Hemoglobin (HGB); (c) Mean corpuscular volume (MCV); (d) Hematocrit (HCT); (e) Mean corpuscular hemoglobin (MCH); (f) Platelet distribution width (PDW); (g) White blood cell (WBC); (h) Red blood cell (RBC); (i) Lymphocyte (Lymph); (j) Red blood cell distribution (RDW); (k) Monocyte (MON); (l) Neutrophilic granulocyte (GRAN).

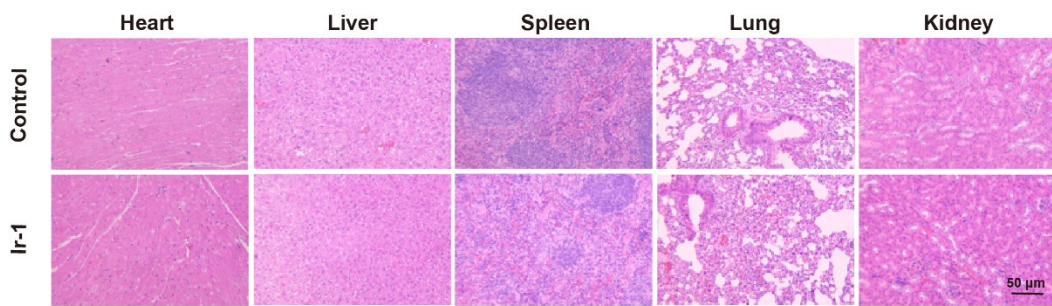


Fig S19. In various treatment groups, H&E-stained sections of mice organs including heart, liver, spleen, lung, and kidney tissues.

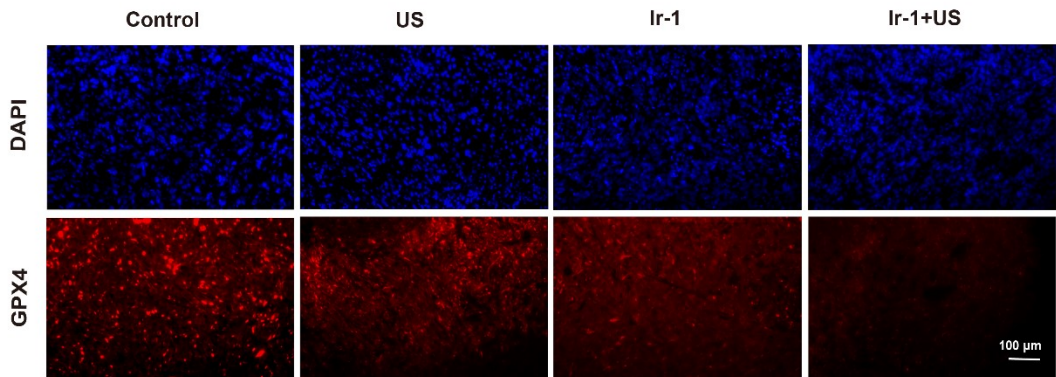


Fig S20. Fluorescence images of 4T1 cells under various treatments.

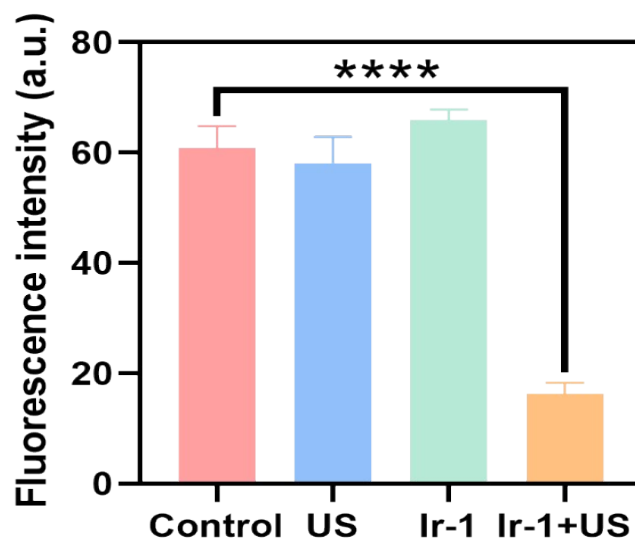


Fig S21. Fluorescence intensities of 4T1 cells under various treatments.

Table S1. The electrochemical properties of **Ir-1** in anhydrous acetonitrile at 298 K.

| | $E_{\text{onset}}^{\text{ox}} (\text{V})^a$ | $E_{\text{onset}}^{\text{red}} (\text{V})^a$ | $E_{\text{HOMO}} (\text{eV})^b$ | $E_{\text{LUMO}} (\text{eV})^c$ | $\Delta E_{\text{gap}} (\text{eV})^d$ |
|-------------|---|--|---------------------------------|---------------------------------|---------------------------------------|
| Ir-1 | 1.016 | -1.301 | -5.416 | -2.975 | 2.441 |

^a Oxidation and reduction potentials measured *via* cyclic voltammetry.

$$^b E_{\text{HOMO}} = - (E_{\text{onset}}^{\text{ox}} + 4.4) \text{ eV}$$

$$^c E_{\text{LUMO}} = E_{\text{HOMO}} + \Delta E_{\text{gap}}$$

$$^d \Delta E_{\text{gap}} = 1240 / \lambda, \lambda \text{ was estimated from the UV-vis absorption spectra.}$$